Time Transfer by Laser Link (T2L2) in Noncommon View Between Europe and China

Etienne Samain, Giovanni Daniele Rovera, *Senior Member, IEEE*, Jean-Marie Torre, Clement Courde, Alexandre Belli, Pierre Exertier, Pierre Uhrich, Philippe Guillemot, Robert Sherwood, Xue Dong, Xingwei Han, Ziang Zhang, Wendong Meng, and Zhongping Zhang

***Abstract*— The Time Transfer by Laser Link (T2L2) project allows for the synchronization of remote ultrastable clocks over intercontinental distances. The principle is derived from the satellite laser ranging technology with a dedicated space equipment designed to record arrival times of laser pulses at the satellite. The space segment was launched in 2008 as a passenger instrument on the ocean altimetry satellite Jason 2. For the first time, we have conducted by the end of 2016 a dedicated time transfer comparison campaign between Global Positioning System and T2L2 over intercontinental distances. The campaign was carried out between two laboratories in Europe and two in China. The campaign has demonstrated a consistency of the time transfer techniques at the 1-ns level, together with the confirmation of a subnanosecond level for continental distances.**

***Index Terms*— Global Positioning System (GPS) common views (CV), laser link, laser ranging, time transfer, time transfer by laser link (T2L2), timescales, uncertainty.**

I. Introduction

GLOBAL Positioning System (GPS) and two-way satellite time and frequency transfer are the most common techniques currently used to achieve comparisons between remote clocks and distributions of time and frequency references.

The time transfer by laser link (T2L2) experiment [1]–[3] aims at achieving time transfer between remote clocks using laser pulses instead of a microwave link. The principle is based upon laser telemetry technology [4] with a network of laser stations on the ground and a dedicated space equipment designed to record arrival time of laser pulses at the satellite. It was developed by the Géoazur Laboratory of Observatoire de la Côte d'Azur, Valbonne, France, with the support of the French Space Agency CNES.

Manuscript received September 28, 2017; accepted February 3, 2018. Date of publication February 8, 2018; date of current version June 1, 2018. *(Corresponding author: Giovanni Daniele Rovera.)*

E. Samain, J.-M. Torre, C. Courde, A. Belli, and P. Exertier are with CNRS, IRD, University Nice Sophia Antipolis, Observatoire de la Côte d'Azur, 069005 Caussols, France (e-mail: etienne.samain@oca.eu).

G. D. Rovera and P. Uhrich are with LNE-SYRTE, Observatoire de Paris, PSL Research University, CNRS, Sorbonne Universités, UPMC University, 75014 Paris, France (e-mail: daniele.rovera@obspm.fr).

P. Guillemot is with CNES, French Space Agency, 31401 Toulouse, France.

R. Sherwood is with NERC Space Geodesy Facility Herstmonceux Castle, Hailsham BN27 1RN, U.K.

X. Dong, X. Han, and Z. Zhang are with Changchun Observatory, NAO, CAS, Changchun 130117, China.

W. Meng and Z. Zhang are with Shanghai Astronomical Observatory, CAS, Shanghai 200030, China.

Digital Object Identifier 10.1109/TUFFC.2018.2804221

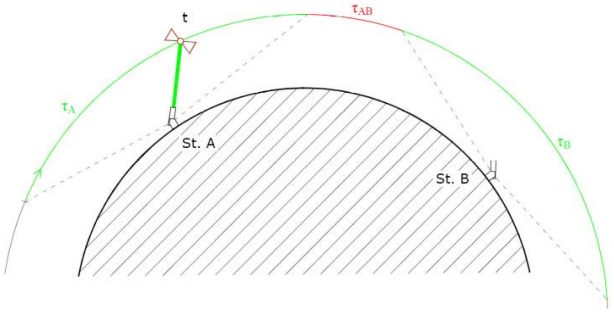

Fig. 1. Non-CV mode. Jason 2 is in line of sight from stations A and B during τ_A and τ_B, respectively. It is not reachable during the period τ_{AB}.

T2L2 benefits from the optical domain with a high modulation bandwidth (5–30 GHz, depending on the duration of the laser pulse) and little sensitivity to ionosphere (<1 ps), and also from the two-way technique on a monocarrier scheme. T2L2 was launched in June 2008 as a passenger instrument on the Jason 2 satellite designed to study the internal structure and dynamics of ocean currents. The full accuracy of the T2L2 link is achieved when the satellite is visible from both ground stations of the link in the common view (CV) mode. The T2L2 experiment has proved to be a very efficient tool for transferring time between the remote ultrastable clocks with a time stability of a few picoseconds over hundreds of seconds and an accuracy at the subnanosecond (ns) level. The results of the direct comparison between T2L2 and GPS CV on continental links lead to a consistency below 250 ps, both techniques having been calibrated independently [5]–[7]. The satellite being at an altitude of 1335 km, the time transfer over intercontinental distances (>5000 km) can only be in a non-CV mode (Fig. 1). In such a configuration, the performance is crucially depending on the stability of the on-board oscillator of the space instrument [8]. In the Jason 2 context, the time reference is the quartz oscillator [9] of the DORIS navigation system, which is used for both DORIS and T2L2.

Up until now, T2L2 had never been compared with other time transfer techniques in such a non-CV configuration. In order to experimentally validate the concept, we decided to carry out a dedicated time transfer comparison campaign between T2L2 and GPS in this non-CV mode over intercontinental distances, both techniques being calibrated independently.

0885-3010 © 2018 IEEE. Translations and content mining are permitted for academic research only. Personal use is also permitted, but republication/redistribution requires IEEE permission. See http://www.ieee.org/publications_standards/publications/rights/index.html for more information.

TABLE I
STATION CHARACTERISTICS

Station	Country	ID	Clock	GPS
Grasse	France	7845	H-Maser Steered to UTC	Dicom GTR50
Herstmonceux	United Kingdom	7840	H-Maser Free Running	Septentrio PolaRX 3
Changchun	China	7237	H-Maser Free Running	Trimble NetR9
Shanghai	China	7821	GPS=DO	Trimble NetR9

TABLE II
LASER CHARACTERISTICS

Station	Telescope Diameter RX/TX (mm)	Laser Energy (mJ)	Lases rate (Hz)	Laser FWHM (ps)
Grasse	1540	200	10	150
Herstmonceux	500/100	1	1000	10
Changchun	600/210	0.8	1000	50
Shanghai	600/210	1	1000	30

The campaign was carried out from June to December 2016 between two laser ranging stations in Europe and two stations in China (Tables I and II). The campaign allowed to compare both non-CV configurations between Europe and Asia and also CV configuration in Europe, the goal there being to try to confirm the previous results. Due to a technical issue and adverse weather conditions, there are no useful data from Shanghai station.

II. T2L2 TIME TRANSFER

A. Presentation

A T2L2 ground-to-ground time transfer between two remote stations is made from individual links between each station and the space segment. The satellite segment is only used as a relay between earth stations. Laser stations emit light pulses of width between 20 and 200 ps toward the satellite. A laser ranging array on-board the satellite returns a fraction of the received pulses to the ground station. The ground station measures, for each laser pulse, the start epoch t_e and the return epoch t_r after reflection from the space. The T2L2 payload records, in the timescale of the space oscillator, the arrival epoch on-board t_b.

B. Common View and Noncommon View Time Transfer

The time transfer can be realized either in a CV or in a non-CV configuration. In the first case, the satellite is seen during a common period, while in the other case the satellite is observed alternatively. In the CV mode, the space oscillator is only solicited over the time interval of laser pulses (typically from 0.1 s to a few seconds) and the noise added by the oscillator itself can be neglected. Over longer periods, the noise

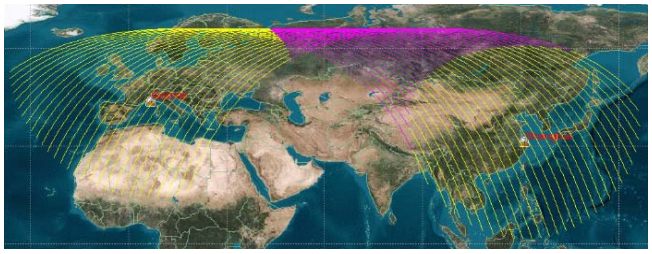

Fig. 2. Jason 2 passes above Europe and Asia. The purple tracks indicate that the satellite is not visible neither by the Grasse station nor by the Shanghai station.

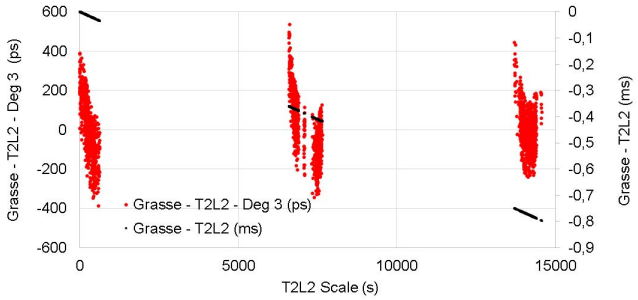

Fig. 3. Example of a ground-to-space time transfer obtained over the Grasse station. Black dots: time offset between the ground clock and the space clock for three consecutive passes. Red dots: difference between this time offset and a polynomial of order 3 fitted on the time offset.

is common for both stations and the difference vanishes. The T2L2 time transfer Δ_{AB} between A and B is computed from each ground-to-space time transfer Δ_{AS} and Δ_{BS}

$$\Delta_{AB} = \Delta_{AS} - \Delta_{BS}. \tag{1}$$

In the non-CV mode, the behavior of the space oscillator has to be considered in its operating environment over the time interval τ_{AB} during which the satellite is not visible neither by A nor by B. Fig. 2 is an illustration of Jason 2 that passes above Europe and Asia: the satellite is visible from the ground over yellow tracks and not visible over pink tracks. The mean value of the nonvisibility period between Europe and Asia is roughly $\tau_{AB} = 1300$ s. For the most favorable track, the values were 960 and 1500 s in the worst case. The behavior of the space oscillator can be taken into account by a correction model C_{Osc}. One has in the non-CV mode

$$\Delta_{AB} = \Delta_{AS} - \Delta_{BS} + C_{Osc}. \tag{2}$$

If the satellite loops over the same ground station at each revolution, the low-frequency noise of the space oscillator can be easily removed with a low-order polynomial determined to fit the ground clock of the station (Fig. 3). Because the ground clock is based on an H-Maser steered to UTC, we assume this signal to be noise free as compared to the on-board clock. Fig. 3 is an example of the measured time offset caused by the satellite clock drift for three consecutive satellite passes. For a given time transfer between A and B, the C_{Osc} value is deduced from a polynomial of degree 3 $P_{Osc}(\tau)$, fit from passes acquired with station A before and after the passes acquired with station B. Terms Δ_{AS} and Δ_{BS} take into account some corrections for general relativity. These corrections are

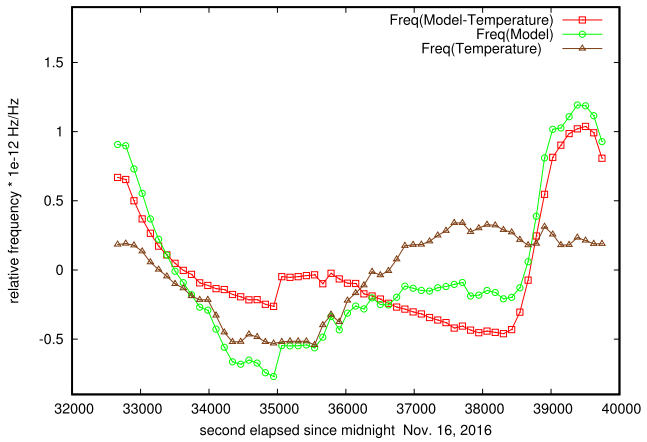

Fig. 4. Model of DORIS instantaneous normalized frequency evolution over a complete revolution of Jason 2. Brown: temperature contribution. Red: radiation contribution. Green: both the temperature and radiation contributions. The long-term time offset was removed on this model.

calculated from the Jason 2 ephemerides and from the International Terrestrial Reference Frame (IRTF2008) solution, giving coordinates with uncertainties of both the laser station and the satellite in the range of a few centimeters, leading to a negligible time transfer uncertainty.

For duration shorter than one orbital period, it is necessary to consider the intrinsic noise of the oscillator (the noise measured in a quiet environment) and also all the systematical phenomena which can disrupt the oscillator. These phenomena are as follows:

1) radiation, which is not constant along the satellite trajectory (South anomaly Atlantic South);
2) temperature, which varies as a function of the Sun position (roughly 0.1 °C over a classical orbit).

A significant part of these systematic perturbations can be removed from a model of the quartz oscillator [10]. Fig. 4 shows the representation of the instantaneous normalized frequency $y(t)$ extracted from this model over a complete revolution of a typical track passing over Europe and Asia. Variations of $y(t)$ functions for all the tracks "Europe–Asia" are not really significant. As a consequence, these systematic frequency perturbations can be modeled as a simple constant M_{Osc} equal to the integral of the frequency bias between τ_{A} and τ_{B}. One has in the non-CV mode

$$M_{\mathrm{Osc}}(\tau_{\mathrm{AB}}) = \int_{\tau_A}^{\tau_B} y(t)dt. \tag{3}$$

Numerically, one has

$$M_{\mathrm{Osc}}(\tau_{\mathrm{AB}}) = -150 \text{ ps}.$$

Finally, the complete contribution coming from the oscillator for the time transfer between A and B is given by

$$C_{\mathrm{Osc}}(\tau_{\mathrm{AB}}) = P_{\mathrm{Osc}}(\tau_{\mathrm{AB}}) + M_{\mathrm{Osc}}(\tau_{\mathrm{AB}}). \tag{4}$$

C. T2L2 Calibration

A classical laser station is an equipment designed to measure accurate distances between a reference point at the ground

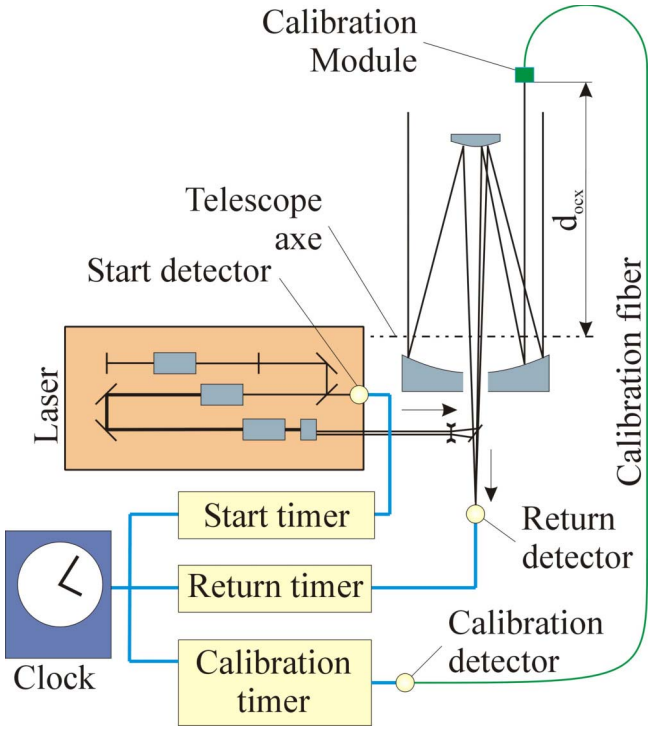

Fig. 5. Laser station during the calibration process. The calibration station includes an event timer (STX301), an optical module, an optical fiber, and an ultrafast detector. The internal calibration of the station is not shown in this figure.

(the cross axes of the telescope) and the observed target (corner cubes on-board the satellite). These distances are computed from the time interval between the start event t_e, corresponding to the emission of the laser pulse, and the stop event t_r, corresponding to the return of the pulse after being reflected by the satellite. Laser stations are regularly calibrated (internal calibration) in order to make this time interval accurate, but this internal calibration is not sufficient for T2L2 since start times of each laser pulse need to be known accurately at sub-ns level [11].

This means that one needs to know at this level of uncertainty the delay between the optical pulse at the cross axis of the telescope and the electrical temporal reference of the station (time distribution unit). The calibration is evaluated for all the participating stations with a traveling calibration equipment. It includes a SigmaTime STX301 subpicosecond event timer, an optical module to grab laser pulses from the laser station and an optical fiber (Fig. 5). The optical module comprises a collimation optic connected to a 50-m monomode optical fiber at 532 nm. This optical module is fixed at the output of the telescope that used to transmit the laser at a given distance d_{Ocx} (δ_{Ocx} when converted in time) from the cross axis of the telescope. The calibration is based on a set of time measurements done between the normal chronometry of the laser station and the traveling T2L2 calibration equipment. We get from these measurements, a mean value of the difference $\delta_{\mathrm{cal-sta}}$ between epochs obtained by the station and the epochs obtained by the calibration station. Knowing the absolute delay δ_{cal} of the calibration station [optical fiber delay,

detector delay, pulse per second (PPS) and photodetector cable delays, and optical module delay], it allows for the delay between the optical pulse at the cross axis of the telescope and the electrical reference of the PPS distribution unit to be known accurately. Finally, start epochs given by the laser station are corrected by

$$\delta_{\mathrm{CalCor}} = \delta_{\mathrm{Cal-Sta}} - \delta_{\mathrm{ocx}} + \delta_{\mathrm{Cal}}. \tag{5}$$

A dedicated calibration operation was organized during the campaign at each of the four participating stations. A last calibration was performed again on the first calibrated laser station after the campaign in order to evaluate a potential drift of the calibration station. The difference between the two calibrations was only 17 ps and can be considered as a negligible drift.

D. T2L2 Error Budget

The T2L2 error budget was studied in detail for time transfer in CV [11]. For a time transfer Δ_{AB} between two ground stations A and B, the combined uncertainty $u_c(\Delta_{\mathrm{AB}})$ is given as

$$u_c^2(\Delta_{\mathrm{AB}}) = u_c^2(\Delta_{\mathrm{AS}}) + u_c^2(\Delta_{\mathrm{BS}}) + u^2(C_{\mathrm{Osc}}(\tau_{\mathrm{AB}})) \tag{6}$$

where $u_c(\Delta_{\mathrm{AS}})$ and $u_c(\Delta_{\mathrm{BS}})$ are the combined uncertainties of the ground-to-space links, and $u[C_{\mathrm{Osc}}(\tau_{\mathrm{AB}})]$ is the uncertainty introduced by the on-board oscillator along the track AB over the duration τ_{AB}. These uncertainties are evaluated from several tens of parameters coming from the laser station instrumentation, the satellite instrument, the atmosphere, and also from the T2L2 calibration.

Uncertainties coming from laser stations should be determined on the precise experimental setup for each link. In order to give a more general uncertainty budget, [11] has defined a typical setup reflecting characteristics of a large number of laser stations well suited for time transfer. The four stations involved in the campaign fall inside these characteristics. The uncertainty given by [11] is

$$u_c(\Delta_{\mathrm{AS}}) = u_c(\Delta_{\mathrm{BS}}) = 98 \text{ ps} \quad (k = 2).$$

The oscillator uncertainty $u[C_{\mathrm{Osc}}(\tau_{\mathrm{AB}})]$ can be estimated from the time deviation $\sigma_{xOsc}(\tau_{\mathrm{AB}})$ of the DORIS oscillator over the duration τ_{AB} measured in a quiet environment and from the noise σ_{QM} of the quartz oscillator model (radiation and temperature). One has

$$u^2(C_{\mathrm{Osc}}(\tau_{\mathrm{AB}})) = \sigma_{xOsc}^2(\tau_{\mathrm{AB}}) + \sigma_{\mathrm{QM}}^2. \tag{7}$$

The time deviation $\sigma_{xOsc}(\tau_{\mathrm{AB}})$ can be computed from the Allan variance of the DORIS oscillator which was measured before the Jason 2 launch (Fig. 6). For the nonvisibility period τ_{AB} applied to the Europe–China time transfer, we have

$$\tau_{\mathrm{AB}} = 1300 \text{ s}.$$

And we get from Fig. 6 (purple curve)

$$\sigma_{x\mathrm{Osc}}(\tau_{\mathrm{AB}}) = \sigma_{x\mathrm{Osc}}(1300) = 650 \text{ ps}.$$

The DORIS oscillator was compared to an atomic clock HP5071A during the final assembly of the T2L2 equipment

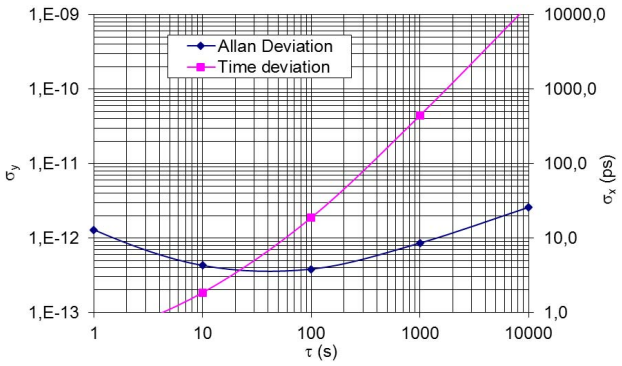

Fig. 6. Allan deviation σ_{yOsc} and time deviation σ_{xOsc} computed and extrapolated from measurements made before the Jason 2 launch.

on-board the Jason 2 spacecraft [12]. The time deviation measured at that time computed for $\tau = 1300$ s is in a good agreement with the value $\sigma_{x\mathrm{Osc}}(1300) = 650$ ps. The noise σ_{QM} has been evaluated [10] from the integration of the oscillator model over several revolutions above the same laser station. One has over the track Europe–Asia

$$\sigma_{\mathrm{QM}} = 300 \text{ ps}.$$

The global uncertainty of the whole time transfer by T2L2 taking into account the uncertainties of ground-to-space time transfers and of the on-board oscillator is then

$$u_c(\Delta_{\mathrm{AB}}) = 730 \text{ ps}.$$

E. T2L2 Experimental Acquisition

Due to some experimental issues at earth stations, usable data were obtained during the two months of November and December 2016. These data represent potentially 380 observable passes over Europe and 250 passes over Asia. The distance between Grasse and Herstmonceux being in the range of 1000 km and the altitude of Jason 2 being 1335 km, most of Jason 2 passes were visible in CV from both stations. For the non-CV configuration, 160 passes were potentially visible from the four laser stations in a direct mode configuration (direct satellite track from Europe to Asia). Taking into account the observation conditions at the ground for all the four stations (availability of observers, weather conditions, and technical problems), we obtained during that campaign:

1) 419 566 laser events detected on-board Jason 2;
2) 180 passes from all stations;
3) 18 passes in non-CV (direct mode);
4) 24 passes in CV (Europe);
5) 6 passes in CV (Asia).

The calibration tour of the four laser stations was undertaken during the acquisition phase of the whole campaign. The calibration operations summary is listed in Table III.

III. GPS Time Transfer

Several methods can be used to compare remote timescales by using signals broadcast by GPS satellites. The so-called TAIP3 technique is based on the P-codes. It was originally

TABLE III
T2L2 CALIBRATION OF THE FOUR PARTICIPATING LASER STATIONS. ALL VALUES ARE IN PICOSECOND

Station	Grasse	Herst.	Chang.	Shanghai	Grasse
Date	09/08/16	08/09/16	16/11/16	07/11/16	01/02/17
δ_{Cal}	-241959	-241959	-241959	-241959	-241959
δ_{Ocx}	12044	2812	3186	3166	12044
$\delta_{Cal-Sta}$	633893	552205	104713	102517	633876
$\delta_{CalCorr}$	379890	307434	-140432	-142608	379873

implemented for the comparison of the clocks contributing to the Temps Atomique International (TAI) [13]. After years of continuous improvement on calibration techniques, the TAIP3 CV allows for time comparisons within an uncertainty of about 1 ns on a freshly calibrated link. Unfortunately, over transcontinental distances, the number of CV can be very low or even zero. For long-distance remote clock comparisons, a method using the same combination of P1 and P2 codes to get the iono-free P3 was developed. It uses all the satellites in view of each station to compute the offset between each local timescale and the GPS timescale (GPST), on its best representation IGST computed by the International GNSS service (IGS). Remote time transfer between two stations is computed as the difference between such data at the same epoch. This all-in-view technique uses the same hardware calibration values as the CV, but in this case the uncertainty on the satellite orbits and clocks should also be taken into account.

Another geodetic technique, generally known as precise point positioning (PPP), is based not only on the P-codes but also on the carrier phase processing, improving significantly the noise of the time transfer. A software developed by the Natural Resources Canada (NRCan) [14] was kindly licensed to SYRTE. Although it is possible to have a few satellites in CV between Europe and China, the TAIP3 CV links are very noisy because of the low number of satellites in common visibility. Therefore, we did compute a calibration offset for the PPP links between the involved stations. We used the same setup as for the classical calibration described in [6]. But instead of evaluating separately the P1 and P2 delays for the receivers, we used a global approach by computing the time differences between the internal time base of each receiver and IGST. The only difference between the PPP link calibration and the TAIP3 CV calibration is the fact that the delays [T_x-GPST] are not evaluated separately for P1 and P2 codes, but globally using the PPP technique. In this case, [6, eqs. (6) and (7)] can be rewritten in the following form:

$$D_A = [T_A - \text{IGST}]_{RA} - [T_A - \text{IGST}]_{\text{MRA}} + RD_{\text{MRA}} \quad (8)$$

$$D_B = [T_B - \text{IGST}]_{RB} - [T_B - \text{IGST}]_{\text{MRB}} + RD_{\text{MRB}} \quad (9)$$

$$\text{Link\_Delay}_{\text{AB}} = D_A - D_B \quad (10)$$

where

1) T_x local time at station x;
2) $[T_x - \text{IGST}]_{\text{Rx}}$ difference between the local time at station x and IGST computed by the PPP process using the data of receiver Rx;
3) $[T_x - \text{IGST}]_{\text{MRx}}$ difference between the local time at station x and IGST computed by the PPP process using the data of the moving receiver MRx;
4) RD_{MRx} measured time difference between the reference point of the traveling receiver in station x and the local timescale reference point.

The calibration achieved this way is very simple, the only drawback is the fact that the calibration would be lost for any change in the hardware setup of a station.

Note that the reduced noise of the PPP will not allow for a more accurate time transfer than the classical TAIP3 CV because the GPS carrier phase does not have a well-defined time tag and is only used to smooth the code noise. In addition, the noise is generally far from being the limiting factor of a calibration uncertainty budget. For this campaign, we used two Septentrio PolaRx 4, OPM3 and OPM7, as well as a choke-ring antenna. Because there was no significant discrepancy neither between the two traveling receivers during all the calibration trips nor for the closure against the reference receiver of the campaign, we can claim for the link Grasse–Herstmonceux the same uncertainty as the one obtained for the best link presented in [6], 1.5 ns ($k = 2$).

For the links involving Changchun, an additional line in the uncertainty budget has to be considered to take into account the instability of the coaxial line linking the building where the reference H-Maser and the local GPS station are located to the building where the satellite laser ranging station and the GPS traveling receivers are implemented. We estimated this instability at about 0.5 ns. For the links involving the Shanghai Astronomical Observatory, it was unfortunately impossible to compute consistent calibration values due to a technical issue with the local oscillator.

The expected expanded uncertainties ($k = 2$) of the three GPS links presented here are as follows:

1) Grasse–Herstmonceux: 1.5 ns for both TAIP3–CV and PPP;
2) Grasse–Changchun: 1.8 ns for PPP only;
3) Herstmonceux–Changchun: 1.8 ns for PPP only.

IV. TIME COMPARISONS

In each visited station, both GPS and T2L2 hardware delays were calibrated against the connector chosen as local timescale reference point. This way, the timescale differences measured between remote stations is expected to be the same when obtained from GPS or T2L2. The sub-ns consistency between both techniques was already demonstrated with T2L2 in CV and TAIP3 CV links [5]. Such former CV results are confirmed here, and we also validate the T2L2 time transfer in non-CV together with the specific calibration of PPP GPS links.

A. Herstmonceux–Grasse

The calibration of the Herstmonceux station was achieved at the beginning of September 2016. But the actual operation of T2L2 did only start in November and lasted up to mid-December. During this period, 21 T2L2 passages have given useful results. The GPS time transfer was computed over the same period of time, both by TAIP3 CV and PPP

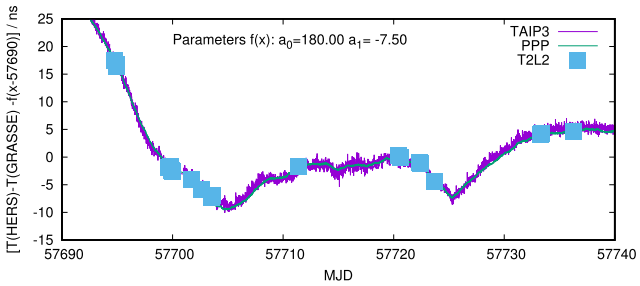

Fig. 7. Time differences in nanosecond between Herstmonceux and Grasse. Violet line: TAIP3 CV. Green line: PPP. Blue squares: T2L2.

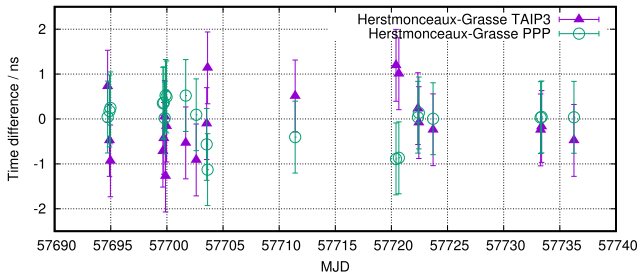

Fig. 8. Differences in nanosecond between techniques on the Herstmonceux–Grasse links. Violet triangles: T2L2–TAIP3 CV. Green circles: T2L2–PPP. For each T2L2 epoch, the GPS time difference is obtained by simple interpolation of the two adjacent GPS points, either TAIP3 or PPP.

techniques. The time differences between Herstmonceux and Grasse timescales are reported in Fig. 7 with a linear drift removed. The violet line is the TAIP3 CV, the much less noisy green line is the PPP and blue squares are the T2L2 points.

The differences between T2L2 and the two GPS techniques are shown in Fig. 8, with the error bars representing the combined uncertainty. In both cases, the average of the differences is below 100 ps and is totally negligible with respect to the combined uncertainty. As expected, the standard deviation of the TAIP3 is bigger than the standard deviation of PPP.

B. Changchun–Grasse

The calibration of the Changchun station took place at the beginning of November 2016 and we had the luck to obtain some useful T2L2 data when the traveling calibration equipment were implemented there. Thanks to this opportunity we also had the possibility to compare the T2L2 time transfer with the TAIP3 CV by using the data of one of the traveling receivers. Unfortunately, the geodetic GPS receivers installed in the Chinese stations, although excellent for geodesy, are not allowing for the generation of Common GNSS Generic Time Transfer Standard (CGGTTS) data required for the TAIP3 CV. For this link, six useful T2L2 time comparison points are available, five of them during the calibration period on site and one at the end. The overall view of the time transfer is displayed in Fig. 9 with a quadratic fit removed, by using the same symbol conventions as above. Due to the instability of the H-Maser in Changchun, the vertical scale is larger than that in the other figures, and the consistency between the techniques is not clearly visible. The more detailed Fig. 10 only covers the period of the presence of the traveling GPS receivers in

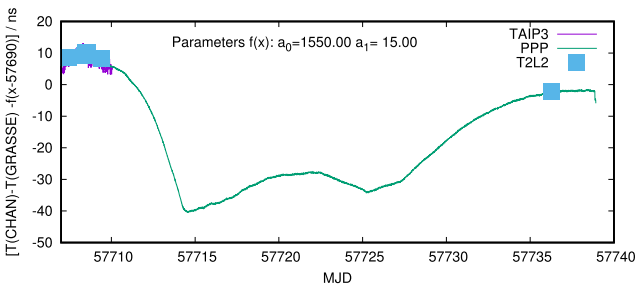

Fig. 9. Time differences in nanosecond between local timescale reference points in Changchun and in Grasse with a quadratic fit removed. Violet line: TAIP3 CV. Green line: PPP. Blue squares: T2L2.

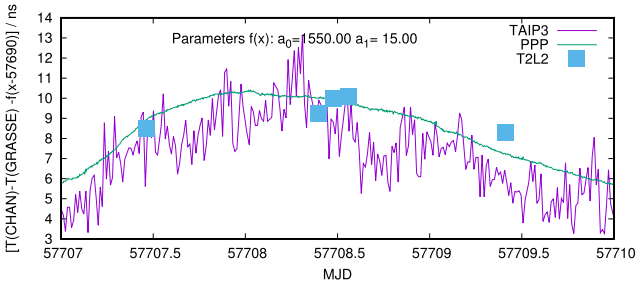

Fig. 10. Time differences in nanosecond between local timescale reference points in Changchun and in Grasse with a quadratic fit removed. Violet line: TAIP3 CV. Green line: PPP. Blue squares: T2L2.

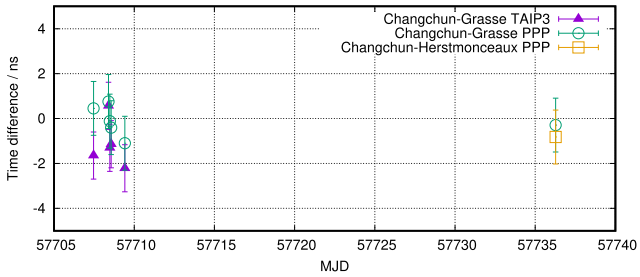

Fig. 11. Differences in nanosecond between time comparisons achieved by T2L2 and GPS. Violet triangle: TAIP3. Green circle: PPP. Orange square: single point obtained on the link Changchun–Herstmonceux.

Changchun. We can obviously see here that GPS PPP and T2L2 are in good agreement, while the TAIP3 CV using one of the traveling receivers differs from T2L2 results by about 1 ns. This discrepancy is also clearly appearing in the plot of the time differences in Fig. 11. Although the differences are staying close to 0 according to the combined uncertainty, this discrepancy suggests that, as expected, the distance between the stations is too large for a proper use of TAIP3 CV.

C. Changchun–Herstmonceux

Due to adverse meteorological conditions, it was only possible to obtain on this link a single T2L2 point at the end of the campaign. This single point, leading to one single T2L2 GPS difference, is also plotted in Fig. 11. It happens to be consistent with the expected results in comparison with the other Europe–China link.

TABLE IV
MEAN VALUES OF THE TIME DIFFERENCES BETWEEN T2L2 AND GPS

Link	Number of points	Mean value (ns)	Standard Deviation (ns)	Combined Uncertainty (ns)
Hers-Grasse TAIP3	21	-0.09	0.67	0.8
Hers-Grasse PPP	21	-0.03	0.46	0.8
Chan-Grasse TAIP3	5	-1.15	0.93	1.2
Chan-Grasse PPP	6	-0.12	0.60	1.2
Chan-Hers PPP	1	-0.82	n.a	1.2

D. Global Results

The average of the time differences between the three links that have produced exploitable results is reported in Table IV. For all the links, the difference between T2L2 and GPS is much lower than the combined uncertainty, except for the TAIP3 link Chanchun–Grasse.

V. CONCLUSION

For the first time T2L2 was demonstrated over intercontinental distances. Such long distance links cannot be realized in CV of the satellite, which means that the on-board oscillator has to be considered properly. A direct comparison of T2L2 results with GPS time transfer was achieved thanks to a GPS PPP link calibration technique. Both techniques having been calibrated independently, the T2L2–GPS differences obtained over the links between Europe and China are all clearly in line with the estimated combined uncertainties, which are close to the 1-ns level.

In addition, the T2L2–GPS differences were also computed over the European link between Grasse and Herstmonceux, after achievement of independent link calibrations. Even by using a completely different GPS traveling equipment for the relative link calibration, we again obtained a sub-100-ps mean offset, totally consistent with the former results described in [5]. This fully confirms the state-of-the-art results previously obtained.

This experiment validates together the different GPS relative calibration techniques and the performances of T2L2 over continental or intercontinental distances. Both techniques are confirmed to be excellent candidates for further intercomparisons with new systems, such as BeiDou or Galileo time transfer, or Atomic Clock Ensemble in Space (ACES) microwave ground-to-ground links, or optical fiber links, even over intercontinental distances.

ACKNOWLEDGMENT

The authors would like to thank all the observers who participated to the acquisition of the T2L2 passes on Jason 2 and the Center National d'Etudes Spatiales for the global support to the T2L2 mission.

Product names and model numbers of the equipment are included for reference only. No endorsement or criticism is implied.

REFERENCES

[1] P. Fridelance, É. Samain, and C. Veillet, "T2L2—Time transfer by laser link: A new optical time transfer generation," *Experim. Astron.*, vol. 7, no. 3, pp. 191–207, 1997.

[2] É. Samain *et al.*, "Time transfer by laser link—The T2L2 experiment on Jason-2 and further experiments," *Int. J. Mod. Phys. D*, vol. 17, no. 7, pp. 1043–1054, 2008.

[3] E. Samain, "Clock comparison based on laser ranging technologies," *Int. J. Mod. Phys. D*, vol. 24, no. 8, p. 1530021, 2015.

[4] J. J. Degnan, "Millimeter accuracy satellite laser ranging: A review," in *Contributions of Space Geodesy to Geodynamics: Technology*, D. E. Smith and D. L. Turcotte, Eds. Washington, DC, USA: AGU, 1993.

[5] P. Exertier *et al.*, "Sub-NS time transfer consistency: A direct comparison between GPS CV and T2L2," *Metrologia*, vol. 53, no. 6, p. 1395, 2016.

[6] G. D. Rovera *et al.*, "Link calibration against receiver calibration: an assessment of GPS time transfer uncertainties," *Metrologia*, vol. 51, no. 5, p. 476, 2014.

[7] E. Samain, P. Vrancken, P. Guillemot, P. Fridelance, and P. Exertier, "Time transfer by laser link (T2L2): characterization and calibration of the flight instrument," *Metrologia*, vol. 51, no. 5, p. 503, 2014.

[8] A. Belli, "Transfert de temps otique spatial (mission T2L2/Jason-2). Applications et impacts en Gèodesie," UFR SCIENCES École Doctorale Carnot-Pasteur, Ph.D. dissertation, Univ. Fance-Comtè, Besançon, France, 2017.

[9] A. Auriol and C. Tourain, "DORIS system: The new age," *Adv. Space Res.*, vol. 46, no. 12, pp. 1484–1496, 2010.

[10] A. Belli *et al.*, "Temperature, radiation and aging analysis of the DORIS ultra stable oscillator by means of the time transfer by laser link experiment on Jason-2," *Adv. Space Res.*, vol. 58, no. 12, pp. 2589–2600, 2016.

[11] E. Samain *et al.*, "Time transfer by laser link: A complete analysis of the uncertainty budget," *Metrologia*, vol. 52, no. 2, p. 423, 2015.

[12] E. Samain, D. Alabnèse, P. Guillemot, F. Para, and P. Vrancken, "Essais métrologique modéle de vol T2L2," Observ. la Côte d'Azur, Caussols, France, Tech. Rep. BT2C T2L2J2 Rev 3, 2007.

[13] P. Defraigne and G. Petit, "Time transfer to TAI using geodetic receivers," *Metrologia*, vol. 40, no. 4, p. 184, 2003.

[14] J. Kouba and P. Héroux, "Precise point positioning using IGS orbit and clock products," *GPS Solutions*, vol. 5, no. 2, pp. 12–28, 2001.

Etienne Samain, photograph and biography not available at the time of publication.

Giovanni Daniele Rovera, photograph and biography not available at the time of publication.

Jean-Marie Torre, photograph and biography not available at the time of publication.

Clement Courde, photograph and biography not available at the time of publication.

Alexandre Belli, photograph and biography not available at the time of publication.

Pierre Exertier, photograph and biography not available at the time of publication.

Pierre Uhrich, photograph and biography not available at the time of publication.

Philippe Guillemot, photograph and biography not available at the time of publication.

Robert Sherwood, photograph and biography not available at the time of publication.

Xue Dong, photograph and biography not available at the time of publication.

Xingwei Han, photograph and biography not available at the time of publication.

Ziang Zhang, photograph and biography not available at the time of publication.

Wendong Meng, photograph and biography not available at the time of publication.

Zhongping Zhang, photograph and biography not available at the time of publication.